

N. Yumita · S. Umemura

## Sonodynamic therapy with photofrin II on AH130 solid tumor

### Pharmacokinetics, tissue distribution and sonodynamic antitumoral efficacy of photofrin II

Received: 12 January 2002 / Accepted: 23 August 2002 / Published online: 17 December 2002  
© Springer-Verlag 2002

**Abstract** *Background:* The pharmacokinetics and tissue distribution of photofrin II (PF) and its efficacy in sonodynamic therapy were studied in rats bearing AH130 solid tumors. *Materials and methods:* In order to find the optimum timing of the ultrasound exposure after administration of PF, the PF concentrations in plasma, skin, muscle and tumor were measured and pharmacokinetically analyzed. Antitumor effects were estimated by measuring tumor size. *Results:* Since the highest concentration of PF in tumors occurred 24 h after administration, ultrasound administration 24 h after the intravenous administration of PF was chosen. Ultrasound alone showed a slight antitumor effect, which became increasingly significant as the dose of PF was increased, while PF alone showed no significant effect. *Conclusions:* PF significantly sensitized solid tumors to the antitumor effect of ultrasound in a synergistic manner.

**Keywords** Ultrasound · Photofrin II · AH130 · Sonodynamic therapy

### Introduction

Sonodynamic therapy (SDT) of cancer is based on preferential uptake and/or retention of a sonosensitizing drug in tumor tissues and subsequent activation of the drug by ultrasound. Ultrasound can penetrate deeply into tissues and can be focused into a small region of tumor to activate a sonosensitizing drug. This is a unique advantage when compared to electromagnetic

modalities such as laser beams in the noninvasive treatment of nonsuperficial tumors [8, 9]. Although there have been several reports of the ability of ultrasound to enhance the antitumor effect of porphyrins in cell culture experiments [7, 10, 13, 17], only a few studies of the antitumor effects in solid tumors have been reported.

Recently, we have found that photochemically active porphyrins such as hematoporphyrin (Hp) and the gallium porphyrin complex ATX-70 show significant antitumor effects when activated with ultrasound [18, 20]. Hematoporphyrin derivative (HPD) is a complex mixture of oligomers of Hp and is retained preferentially in tumor tissues much longer than in normal tissues. Its homogeneous form, photofrin II (PF), has been approved by the FDA as a photosensitizer in photodynamic therapy (PDT) of cancer. These are the most widely used sensitizers in PDT in combination with laser irradiation, both in experimental studies and in clinical trials [1, 2, 3, 4, 5].

Although PF is most widely used in PDT, the in vitro ultrasound-induced cell-killing effects of PF have only briefly been reported [11, 12, 13]. Tachibana et al. have observed an enhancement of ultrasound-induced in vitro cell killing [11] and in vivo liver damage [12] in the presence of PF, but the effects on solid tumors have not been reported. It may be important to know whether this FDA-approved sensitizer, PF, shows significant in vivo antitumor effects in solid tumors in combination with ultrasound.

In this study, the in vivo antitumor effect of SDT with PF in AH130 solid tumors was investigated using ultrasound at 2 MHz in standing wave mode. In order to establish the optimum timing for exposure of the tumor to ultrasound, the time courses of PF concentrations in plasma, tumor, muscle and skin were measured and pharmacokinetically analyzed. This is important because these time courses can be different depending not only on the sensitizer but also on the animal species and the tumor cell line [10]. The time courses of the concentration in solid tissues can be

N. Yumita  
School of Pharmaceutical Sciences, Toho University,  
2-2-1 Miyama, Funabashi, Chiba 274-8510, Japan

S. Umemura (✉)  
Central Research Laboratory, Hitachi, Ltd.,  
1-280 Higashi-Koigakubo, Kokubunji, Tokyo 185-8601, Japan  
Tel.: +81-423-231111  
Fax: +81-423-277747

obtained from a minimal number of samples by a pharmacokinetic analysis based on the concentration in blood, for which frequent sampling is much easier. The tumor was exposed to ultrasound at the time when PF concentration in the tumors was maximal.

## Materials and methods

### Chemicals

PF was supplied by Nihon Ledari (Tokyo, Japan). All other reagents were commercial products of analytical grade.

### Tumor cells and animals

AH130 cells were supplied by Meiji Seika Kaisha (Tokyo, Japan). These cell lines were passaged weekly in the form of ascites through 5-week-old male Donryu rats. Cells were harvested from the peritoneal cavity of a tumor-bearing animal 5 to 7 days after inoculation. AH130 cells were suspended in physiological saline solution at a concentration of  $4 \times 10^7$  cells/ml, and 0.1-ml aliquots were subcutaneously inoculated into the left dorsal scapula region of 5-week-old male Donryu rats. The tumors which had grown to approximately 10 mm in diameter by 5 days after inoculation were used in the experiments. The experimental animals were treated according to the guidelines of the Science Council of Japan.

### Determination of PF concentrations in plasma and tissue

PF was dissolved in a sterilized saline solution and administered to tumor-bearing rats at a dose of 5 mg/kg by intravenous injection into the caudal vein. Under pentobarbital anesthesia blood samples were obtained from the femoral artery through a cannula into heparinized tubes 1, 3, 5, 10, 15 and 30 min, and 1, 2, 4 and 6 h after administration of PF. The plasma was separated by centrifugation at 2500 g for 10 min. The animals were killed 2, 6, 24, 48 and 72 h after treatment and the tumor and other tissues were taken immediately. The tissues were excised, blotted dry and weighed. The samples were stored at  $-20^\circ\text{C}$  until use. Plasma (0.2 ml) was mixed with 2.5 ml 10 mM cetyl trimethyl ammonium bromide (CTAB) dissolved in 50 mM 4-(2-hydroxyethyl)-1-piperazinethanesulfonic acid (HEPES) buffer (pH 7.4). A portion of tissue (0.25 g) was homogenized in 2.5 ml of the same buffer. The sample was then shaken with 6 ml of a chloroform/methanol mixture (1:1 v/v) for extraction. After centrifuging at 3000 g for 10 min, the chloroform layer was removed and the aqueous layer was shaken with 3 ml chloroform for the second extraction. The first and second chloroform layers were combined and evaporated to dryness in a water bath at  $30^\circ\text{C}$ . The residue was dissolved in 0.1–1.0 ml methanol. The concentration of PF was determined by measuring the fluorescence intensity using a fluorescence spectrophotometer (model 650-10L; Hitachi, Tokyo, Japan) at an excitation wavelength of 403 nm and an emission wavelength of 628 nm.

### Pharmacokinetic analysis

Pharmacokinetic analysis of the disappearance of PF from the plasma was performed based on a two-compartment open model. The plasma concentration of PF ( $C_p(t)$ ) is described by Eq. 1. The observed plasma concentrations were fitted to Eq. 1, and the pharmacokinetic parameters  $A$ ,  $\alpha$ ,  $B$  and  $\beta$  were determined by a nonlinear least-squares method.

$$C_p(t) = A \exp(-\alpha t) + B \exp(-\beta t) \quad (1)$$

The area under the plasma concentration curve (AUC) from time zero to infinity, the plasma total body clearance ( $CL_{\text{tot}}$ ), and

the distribution volume at steady-state ( $V_{d_{ss}}$ ) are given by the following equations.

$$AUC = A/\alpha + B/\beta \quad (2)$$

$$CL_{\text{tot}} = \text{dose}/AUC \quad (3)$$

$$V_{d_{ss}} = \text{dose}(A\beta^2 + B\alpha^2)/(B\alpha + A\beta)^2 \quad (4)$$

The concentration of PF in tumor ( $C_T(t)$ ) is given by the convolution integral equation:

$$C_T(t) = \int_0^t C_p(t-\theta) \cdot K_1 \exp(-k_2 \theta) d\theta \quad (5)$$

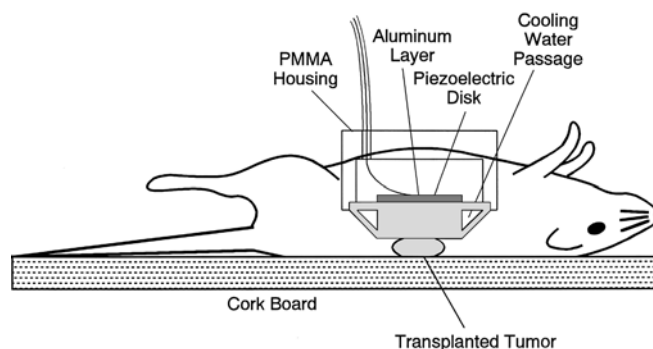
where  $K_1 = k_1 \cdot V_p/V_t$  is the transport clearance of PF to the tissue per unit volume of the tissue. Here,  $V_p$  is the volume of plasma,  $V_t$  is the volume of tissue, and  $k_1$  and  $k_2$  are the first-order rate constants. To estimate  $K_1$  and  $k_2$  by the nonlinear least squares method, the observed tissue concentrations ( $C_T(t)$ ) were curve fitted to Eq. 5 in which  $C_p(t)$  was calculated from  $A$ ,  $\alpha$ ,  $B$  and  $\beta$  [14].

### Ultrasound exposure system

The ultrasound exposure set-up is shown in Fig. 1. A piezoelectric ceramic disk transducer, 24 mm in diameter, was tightly bonded onto an aluminum matching layer, which was cooled by circulating water to keep the transducer and tumor temperature below a certain level. The overall resonant frequency of the transducer was 1.92 MHz. Sine waves were generated by a wave generator (model MG442A; Anritsu, Tokyo) and amplified by an RF amplifier (model 210L; ENI, Rochester, N.Y.). The sinusoidal drive signal of the transducer was monitored by an oscilloscope during ultrasound exposure. In the ultrasound exposure experiments, the transducer was driven at a voltage corresponding to the free-field intensity.

### Treatment protocol

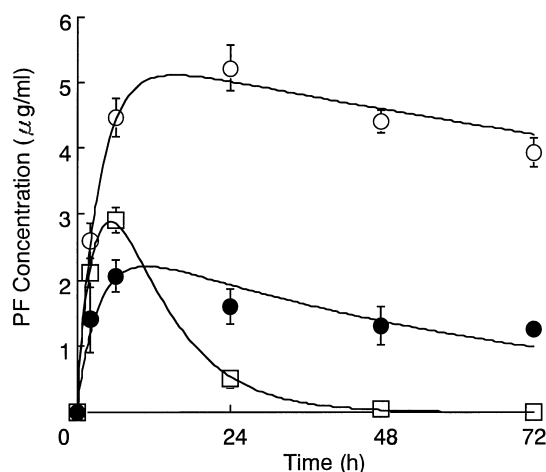
The tumor-bearing rats were divided into four groups of four rats: (1) the control group, and those treated with (2) PF (3) ultrasound, and (4) PF plus ultrasound. PF was administered to rats via the caudal vein. For ultrasound treatment, the rats were anesthetized with sodium pentobarbital (40 mg/kg, i.p.). The hair over the tumors was shaved and ultrasound gel was applied to the naked skin. The rats were fixed to a board with the tumor upwards. The thermistor probe (Anritsu, Tokyo, Japan) was inserted into the tumor to monitor the temperature. The transducer was placed tightly on the tumor, which was exposed to ultrasound for 15 min. The transducer was cooled by a circulating water at  $25^\circ\text{C}$  during the exposure to keep the temperature of the tumor below  $35^\circ\text{C}$ , which is much lower than the hyperthermia level. For the combined treatments, ultrasound was started 24 h after PF administration.



**Fig. 1** Schematic diagram of the ultrasound exposure set-up. A cross-section of the ultrasonic transducer is shown

**Table 1** Pharmacokinetic parameters of PF after intravenous administration calculated from the mean plasma concentration of four rats

Parameter	
A ( $\mu\text{g/ml}$ )	$77.4 \pm 4.4$
$\alpha$ ( $\text{min}^{-1}$ )	$0.145 \pm 0.037$
B ( $\mu\text{g/ml}$ )	$53.9 \pm 28.5$
$\beta$ ( $\times 10^{-3}$ , $\text{min}^{-1}$ )	$4.82 \pm 2.15$
AUC ( $\mu\text{g}\cdot\text{h/ml}$ )	$12,945 \pm 3136$
CL <sub>tot</sub> ( $\times 10^{-3}$ , ml/min/kg)	$0.412 \pm 0.446$
Vd <sub>ss</sub> (ml/kg)	89.1

**Fig. 2** Time course of PF concentrations in tumor and skin after intravenous administration (*open circles* tumor, *open squares* muscle, *closed circles* skin). Each point and vertical bar represents the mean  $\pm$  SD from four rats

#### Evaluation of antitumor effect

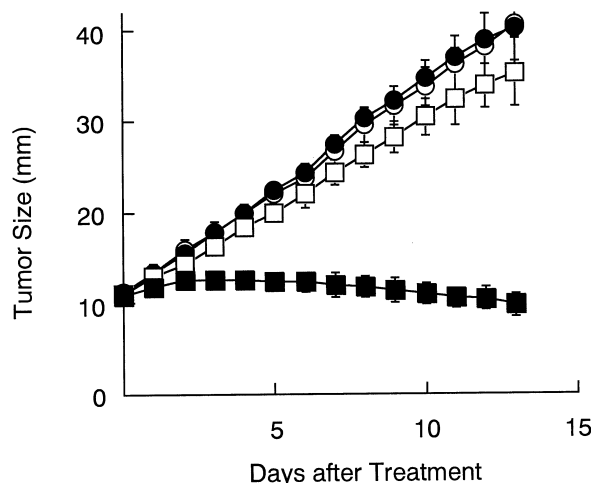
The long and short diameters ( $a$  and  $b$  in millimeters) of the tumors were measured with a slide caliper every day after transplantation. Tumor sizes were calculated as  $(a+b)/2$ . The mean and standard deviation (SD) were calculated for each group. The values were compared using Student's  $t$ -test with 0.05 as the minimum level of significance.

## Results

The concentrations of PF in plasma after intravenous administration were best fitted by the biexponential equation (Eq. 1). The calculated pharmacokinetic parameters are listed in Table 1. The elimination half-life in the terminal phase ( $t_{1/2\beta}$ ) was 144 min. The time courses of the PF concentrations in tumor, skin and muscle are shown in Fig. 2. The parameters representing the distribution of PF to tumor, skin and muscle were calculated using Eq. 5, and are shown in Table 2. The fitting curves for the concentrations in tissues calculated with Eq. 5 and the parameters listed in Table 2 are also shown in Fig. 2. The highest concentration of PF in the tumor was observed 24 h after administration. The PF concentration in the tumor exceeded by an order of magnitude that in the plasma for 24 h or longer after

**Table 2** Pharmacokinetic parameters of PF after intravenous administration

Parameter	Tumor	Muscle	Skin
$K_1$ ( $\times 10^{-4}$ , $\text{min}^{-1}$ )	4.61	4.53	2.19
$K_2$ ( $\times 10^{-3}$ , $\text{min}^{-1}$ )	0.059	1.92	0.236

**Fig. 3** Effect of PF and/or ultrasound on growth of AH130 tumor (*open circles* control, *closed circles* PF alone, *open squares* ultrasound alone, *closed squares* PF plus ultrasound). PF was administered 24 h before ultrasound at a dose of 2.5 mg/kg, and ultrasound was administered at a free-field intensity of 3 W/cm<sup>2</sup>. Each point and vertical bar represents the mean  $\pm$  SD from four rats

administration. The PF concentration in the tumor was significantly higher than in the skin and muscle throughout the experiments.

The effect of each treatment on the growth of AH130 cells is shown in Fig. 3 which indicates the tumor size for 2 weeks after the day of treatment. PF alone at a dose of 2.5 mg/kg had no inhibitory effect. Ultrasound alone at a free-field intensity of 3 W/cm<sup>2</sup> showed a slight inhibitory effect. PF plus ultrasound showed a synergistic antitumor effect such that the tumor size started decreasing 3 days after treatment.

The effect of ultrasound intensity on tumor growth is shown in Fig. 4 for the absence (Fig. 4a) and presence (Fig. 4b) of PF administration at a dose of 2.5 mg/kg. Curves corresponding to free-field ultrasound intensities of 0, 1, 2, 3, and 5 W/cm<sup>2</sup> are shown. An ultrasound intensity threshold for the antitumor effect is clearly seen between free-field intensities of 2 and 3 W/cm<sup>2</sup> in the presence of PF administration (Fig. 4b). At free-field intensities of 3 and 5 W/cm<sup>2</sup>, slight antitumor effects were observed even without PF (Fig. 4a).

The effect of PF dose on tumor growth is shown in Fig. 5. Curves corresponding to PF doses of 0, 0.25, 0.5, 1.0, 2.5, and 5.0 mg/kg with ultrasound exposure at a free-field intensity of 3 W/cm<sup>2</sup> are shown. Without PF, ultrasound showed a slight antitumor effect, which became more significant as the dose of PF increased.

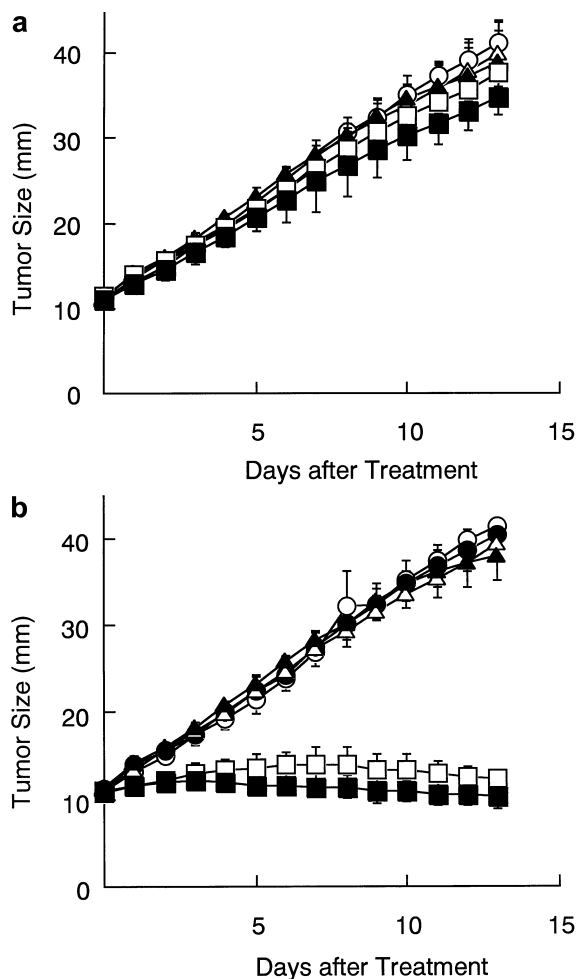


**Fig. 4a, b** Effect of ultrasound intensity on tumor growth (a) in the absence of PF and (b) in the presence of PF at a dose of 2.5 mg/kg. PF was administered alone (open circles) or 24 h before ultrasound at free-field intensities of 1 W/cm<sup>2</sup> (open triangles), 2 W/cm<sup>2</sup> (closed triangles), 3 W/cm<sup>2</sup> (open squares), and 5 W/cm<sup>2</sup> (closed squares). Each point and vertical bar represents the mean ± SD from four rats

## Discussion

SDT for cancer is based on the use of sonosensitizing agents that accumulate relatively selectively in tumors and become cytotoxic when activated by ultrasound. It is reasonable to think that SDT would be most effective if the tumor is exposed to ultrasound when the PF concentration in the tumor is at its maximum. Furthermore, the adverse effects of SDT treatment can be minimized by exposure to ultrasound when the sensitizer concentration in the tumor is significantly higher than in normal tissues [1, 2, 3, 4, 5, 18, 20]. In order to determine the optimum timing for ultrasound exposure, the concentrations of PF in plasma, tumor, muscle and skin were measured and pharmacokinetically analyzed. The PF concentrations in plasma were well explained by a two-compartment open model. The distribution volume ( $V_{d_{ss}}$ ) of PF was 89 ml/kg. This small value suggests

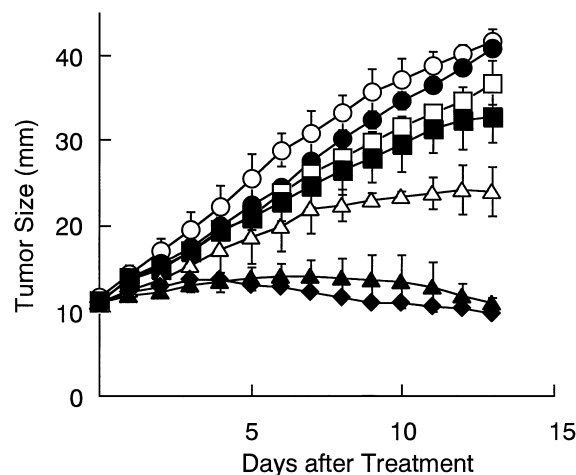


**Fig. 5** Effect of PF dose on tumor growth. PF was administered alone (closed circles) or 24 h before ultrasound at a free-field intensity of 3 W/cm<sup>2</sup>. The PF doses were: 0.25 mg/kg (open squares), 0.5 mg/kg (closed squares), 1.0 mg/kg (open triangles), 2.5 mg/kg (closed triangles), 5.0 mg/kg (closed diamonds). Each point and vertical bar represents the mean ± SD from four rats (open circles control)

that PF does not markedly distribute into tissues. The maximum concentration of PF in the tumor was observed 24 h after administration. At the same time, the PF concentration in the tumor was several times higher than in the plasma and in normal tissues including skin and muscle, as shown in Fig. 4. On the basis of these results, we chose to expose the tumor to ultrasound 24 h after intravenous administration of PF.

The parameters in Table 2 calculated using Eq. 5 represent the transport of PF to the tumor, skin and muscle. The value of  $K_1$  of tumor was only one-tenth that of  $\beta$  of plasma. This means that PF was transported to the tumor much more slowly than it was eliminated from the blood. The accumulation of porphyrin compounds has been reported in a variety of tumors in experimental animals and humans [1, 2, 3, 4, 5, 8]. Recent in vitro and in vivo studies suggest the involvement of specific tumor tissue properties, such as tumor stroma structure, leaky vasculature, poor lymphatic drainage, and an elevated number of low-density lipoprotein (LDL) receptors [2, 6].

When both PF dose and ultrasound intensity were higher than certain levels, significant antitumor effects were observed. Ultrasound intensity seemed to have a relatively sharp threshold, which is typical for ultrasonic effects mediated by acoustic cavitation. A slight antitumor effect was observed even without PF at an ultrasound intensity higher than the threshold. A similar tendency has been observed in an in vitro experiment of ultrasound-induced cell damage with and without PF [21]. These results may imply that the observed ultrasound-induced antitumor effect arises from acoustic cavitation, whether with PF or not. The mechanism of activation of porphyrins by ultrasound has not been fully explained. Umemura et al. have suggested that

sonoluminescence light produced during cavitation collapse of microbubbles is responsible for photoactivation of porphyrins with subsequent formation of singlet oxygen, a known reactive toxic species [15, 16, 17, 19]. Although all these results point to the involvement of acoustic cavitation, further investigation is needed.

The PF dose showed a broader threshold and the antitumor effect gradually increased as the dose increased. At a PF dose not less than 2.5 mg/kg and at a free-field ultrasound intensity not less than 3 W/cm<sup>2</sup>, the synergistic effect between PF and ultrasound on tumor growth inhibition was marked. The observed effective dose of PF is one or two orders of magnitude lower than its lethal dose (LD<sub>50</sub> 150 mg/kg i.v., for mice) [14]. Thus, as the adverse effect of the sonodynamic use of PF, the toxicity of PF alone may be much less important than potential photosensitive dermatitis. From this point of view, the considerable accumulation of PF in the tumor may be an advantage for sonodynamic therapy using PF as a sensitizer.

In conclusion, the results presented suggest that an approved PDT sensitizer, PF, is also a potential sensitizer in sonodynamic tumor treatment. In the pharmacokinetics study, we examined the behavior of PF in tumor-bearing rats and estimated the distribution of PF in tumor tissue in comparison to normal tissues in order to predict the effect of treatment. Our findings have therapeutic implications for the planning of SDT with PF. Since in the treatment study it was confirmed that PF shows an ultrasound-induced antitumor effect as well as tumor selectivity, other porphyrin derivatives should also be tested in the future. The pharmacokinetic approach described here will also be useful in determining the best treatment plans for such agents.

## References

1. Bellnier DA, Ho YK, Panday RK, Missert JR, Dougherty TJ (1989) Distribution and elimination of photofrin II in mice. *Photochem Photobiol* 50:221
2. Dougherty TJ (1993) Photodynamic therapy. *Photochem Photobiol* 58:895
3. Dougherty TJ, Cooper MT, Mang TS (1990) Cutaneous phototoxic occurrences in patients receiving photofrin. *Lasers Surg Med* 10:485
4. Dougherty TJ, Grindery GB, Weishaupt KR, Boyle DG (1975) Photoradiation therapy. II. Cure of animal tumors with hematoporphyrin and light. *J Natl Cancer Inst* 55:115
5. Hayata Y, Kato H, Konaka C, Ono J, Takizawa N (1982) Hematoporphyrin derivative and laser photoradiation in the treatment of lung cancer. *Chest* 81:269
6. Kessel D (1986) Porphyrin-lipoprotein association as a factor in porphyrin localization. *Cancer Lett* 33:183
7. Kessel D, Jeffers R, Fowlkes JB, Cain C (1994) Porphyrin-induced enhancement of ultrasound cytotoxicity. *Int J Radiat Biol* 66:221-228
8. Kremkau FW (1979) Cancer therapy with ultrasound. *J Clin Ultrasound* 7:287
9. Lele PP (1982) Local hyperthermia by ultrasound. In: Nussbaum GH (ed) *Physical aspect of hyperthermia*. American Institute Physics, New York, pp 393-440
10. Mitchell JB, Cook JA, Russo A (1990) Biological basis for phototherapy. Morstyn G, Kay AH (ed) *Phototherapy of cancer*. Harwood Academic Publishers, Chur, p 13
11. Tachibana K, Kimura N, Okamura M, Eguchi H, Tachibana S (1993) Enhancement of cell killing of HL-60 cells by ultrasound in the presence of the photosensitizing drug photofrin II. *Cancer Lett* 72:195
12. Tachibana K, Sugata K, Meng J, Okamura M, Tachibana S (1994) Liver tissue damage by ultrasound in combination with photosensitizing drug, photofrin II. *Cancer Lett* 78:177
13. Tachibana K, Uchida T, Hisano S, Morioka E (1997) Eliminating adult T-cell leukemia cells with ultrasound. *Lancet* 349:9048
14. Takagi H, Harada Y, Misawa N, Inomata N, Liem T, Ilse D (1995) Acute and subchronic toxicities of porfimer sodium (photofrin II) in mice, rats and dogs. *Pharmacometrics* 4:439
15. Umemura S, Yumita N, Nishigaki R, Umemura K (1990) Mechanism of cell damage by ultrasound in combination with hematoporphyrin. *Jpn J Cancer Res* 81:955
16. Umemura S, Yumita N, Nishigaki R (1993) Enhancement of ultrasonically induced cell damage by a gallium-porphyrin complex, ATX70. *Jpn J Cancer Res* 84:582
17. Yumita N, Nishigaki R, Umemura K, Umemura S (1989) Hematoporphyrin as a sensitizer of cell damaging effect of ultrasound. *Jpn J Cancer Res* 80:219
18. Yumita N, Nishigaki R, Umemura K, Umemura S (1990) Synergistic effect of ultrasound and hematoporphyrin on sarcoma 180. *Jpn J Cancer Res* 81:304
19. Yumita N, Nishigaki R, Umemura K, Morse PD, Swartz HM, Cain CA, Umemura S (1994) Sonochemical activation of hematoporphyrin; an ESR study. *Radiat Res* 138:171
20. Yumita N, Sasaki K, Umemura S, Yukawa A, Nishigaki R (1997) Sonodynamically induced antitumor effect of gallium-porphyrin complex by focused ultrasound on experimental kidney tumor. *Cancer Lett* 112:79
21. Yumita N, Umemura S, Nishigaki R (2000) Ultrasonically induced cell damage enhanced by photofrin II: mechanism of sonodynamic activation. *In Vivo* 14:425